THE JOURNAL OF BIOLOGICAL CHEMISTRY VOL. 286, NO. 35, pp. 30471–30480, September 2, 2011

Immunity-related GTPase M (IRGM) Proteins Influence the Localization of Guanylate-binding Protein 2 (GBP2) by Modulating Macroautophagy

Received for publication, April 18, 2011, and in revised form, June 27, 2011 Published, JBC Papers in Press, July 12, 2011, DOI 10.1074/jbc.M111.251967

Maria K. Traver[‡], Stanley C. Henry[§], Viviana Cantillana[¶], Tim Oliver[‖], Julia P. Hunn[**], Jonathan C. Howard[**], Sandra Beer[‡‡], Klaus Pfeffer[‡‡], Jörn Coers[‡], and Gregory A. Taylor[‡§¶§§1]

From the [‡]Department of Molecular Genetics and Microbiology, [§§]Immunology, [‖]Cell Biology, and Medicine, Division of Geriatrics, and [¶]Center for the Study of Aging and Human Development, Duke University, Medical Center, Durham, North Carolina 27710, the [§]Geriatric Research, Education, and Clinical Center, VA Medical Center, Durham, North Carolina 27705, the [**]Institute for Genetics, Department of Cell Genetics, University of Cologne, Cologne 50674, Germany, and the [‡‡]Institute of Medical Microbiology and Hospital Hygiene, Heinrich Heine University of Düsseldorf, Düsseldorf 40225, Germany

The immunity-related GTPases (IRGs) are a family of proteins induced by interferon-γ that play a crucial role in innate resistance to intracellular pathogens. The M subfamily of IRG proteins (IRGM) plays a profound role in this context, in part because of the ability of its members to regulate the localization and expression of other IRG proteins. We present here evidence that IRGM proteins affect the localization of the guanylate-binding proteins (GBPs), a second family of interferon-induced GTP-binding proteins that also function in innate immunity. Absence of Irgm1 or Irgm3 led to accumulation of Gbp2 in intracellular compartments that were positive for both the macroautophagy (hereafter referred to as autophagy) marker LC3 and the autophagic adapter molecule p62/Sqstm1. Gbp2 was similarly relocalized in cells in which autophagy was impaired because of the absence of Atg5. Both in Atg5- and IRGM-deficient cells, the IRG protein Irga6 relocalized to the same compartments as Gbp2, raising the possibility of a common regulatory mechanism. However, other data indicated that Irga6, but not Gbp2, was ubiquitinated in IRGM-deficient cells. Similarly, coimmunoprecipitation studies indicated that although Irgm3 did interact directly with Irgb6, it did not interact with Gbp2. Collectively, these data suggest that IRGM proteins indirectly modulate the localization of GBPs through a distinct mechanism from that through which they regulate IRG protein localization. Further, these results suggest that a core function of IRGM proteins is to regulate autophagic flux, which influences the localization of GBPs and possibly other factors that instruct cell-autonomous immune resistance.

The innate immune system is comprised of multiple effector pathways that are induced in host cells by proinflammatory cytokines such as IFN-γ. Such effectors confer on the host cells the ability to more easily eradicate invading pathogens through diverse mechanisms (1–4). A prominent family of IFN-γ-induced proteins that are required for resistance to intracellular bacteria and protozoa are the immunity-related GTPases. IRG[2] proteins share a number of biochemical functions: they are GTPases (5, 6), they bind lipid membranes in various intracellular membrane compartments (6–8), and they form dimers and/or oligomers (5, 9). These and other characteristics relate them to the dynamins, a large family of GTP-binding proteins that are involved in vesicle formation, vesicle trafficking, and other aspects of lipid membrane remodeling (10–12). Like the dynamins, current models suggest that the IRGs modulate membrane processing in cells (8, 13), which in turn impacts pathogen survival and/or leukocyte functioning.

IRG proteins can be separated into the IRGA, IRGB, IRGC, IRGD, and IRGM subfamilies based on homology across the GTP-binding domain (14). Proteins in the IRGM subfamily are distinguished from the other proteins by possessing a non-canonical GMS sequence in the first GTP-binding motif (G1), whereas the remaining subfamilies all possess the canonical GKS sequence (15). Previous work from our laboratory and others has demonstrated that the IRGM (GMS) proteins play a particularly important role in innate immune resistance to intracellular bacteria and protozoa in mice (8, 14, 16–26). Absence of Irgm1, for instance, leads to a striking susceptibility to multiple organisms, including *Toxoplasma gondii* (8, 19), *Salmonella typhimurium* (25), *Listeria monocytogenes* (19), *Chlamydia trachomatis* (27, 28), and *Mycobacterium* species (20, 21). In comparison, absence of the GKS proteins Irgd or Irga6 results in relatively weak phenotypes (8, 13, 19). The more prominent role for the IRGM/GMS proteins in host resistance can be explained in part by their ability to regulate the expression, localization, and activation of GKS IRG proteins (25, 29, 30). For instance, in Irgm1- and Irgm3-deficient cells, Irga6 and Irgb6 form large aggregate-like structures, decreasing their localization to pathogen-containing vacuoles where they are thought to affect pathogen clearance. However, an open question is whether IRGM proteins possess broader functions that could contribute to the apparent complete absence of IFN-γ-induced host resistance that has been noted against several different pathogens as a result of IRGM deficiency (19–22).

[1] To whom correspondence should be addressed: 508 Fulton St., Rm. N3008, Durham, NC 27705. Tel.: 919-286-0411; Fax: 919-286-6823; E-mail: gregory.taylor@duke.edu.

[2] The abbreviations used are: IRG, immunity-related GTPase; GBP, guanylate-binding protein; TUBE 1, tandem ubiquitin binding entity 1; MEF, mouse embryonic fibroblast; GMS, glycine-methionine-serine; GKS, glycine-lysine-serine; 3T3, 3-day transfer, inoculum 3×10^5 cells.

In this work, we address the possibility of broader regulatory functions by examining whether IRGM proteins can affect the localization and functioning of another important family of IFN-γ-induced effectors, the guanylate binding proteins (GBPs) (31–33). Like the IRG proteins, GBPs can be functionally classified within the dynamin protein superfamily (11, 34) and have been implicated in vacuolar processing and resistance to pathogens such as *T. gondii*, *L. monocytogenes*, and *C. trachomatis* (35, 36). Despite no previous evidence of interactions between these two protein families, we find that the absence of IRGM proteins has striking effects on the localization of GBPs. Our findings suggest that IRGM proteins may have activities that extend beyond the IRG protein family to influence other IFN-γ-induced effectors by modulating autophagy.

EXPERIMENTAL PROCEDURES

Mice and Cell Culture—Irgm1 (LRG-47)-deficient and Irgm3 (IGTP)-deficient mice were generated as described previously (19). The mice were maintained according to Institutional Animal Care and Use Committee-approved protocols at the Durham VA and Duke University Medical Centers (Durham, NC). Mouse embryonic fibroblasts were derived from these mouse lines and immortalized by the standard 3T3 procedure (37). Atg5-deficient fibroblasts were a gift from Herbert Virgin, Washington University, St. Louis, MO. 3T3 fibroblasts were cultured in DMEM (Invitrogen) supplemented with 10% (v/v) FBS (Hyclone, Logan, UT). Twenty-four hours prior to most experiments, 100 units/ml IFN-γ (#407320, Calbiochem, EMD Biosciences, San Diego, CA) was added to the culture medium. Primary bone marrow macrophages were isolated from the tibia and femurs of 2- to 4-month-old mice. Bone marrow was flushed from the bones using a 27-gauge needle fitted to a syringe filled with DMEM, and the marrow was dispersed by drawing through the needle three to four times. Red cells were lysed with ACK lysing buffer (Invitrogen). Adherent cells were cultured for 6 days in bone marrow macrophage medium (culture medium supplemented with 30% (v/v) L929 cell-conditioned culture medium). The cells were cultured on Petri dishes, resulting in cultures that were loosely adherent and easily removed from the plates with cell dissociation buffer (#13150–016, Invitrogen). Twenty-four hours prior to all experiments, the cells were plated on polylysine-coated coverslips in medium lacking L929-conditioned media (DMEM supplemented with 10% (v/v) FBS) containing 100 units/ml IFN-γ.

Immunocytochemistry—Cells were fixed with 4% paraformaldehyde (w/v) in PBS for 15 min, rinsed in 100 mM glycine/PBS for 5 min, and permeabilized with 0.2% (w/v) saponin/PBS for 10 min. Cells were blocked with 10% (v/v) FCS/PBS for 60 min. As indicated in the text, the cells were then stained with various primary antibodies for 60 min, followed by Alexa Fluor-conjugated secondary antibodies (Molecular Probes/Invitrogen) for 60 min. The primary antibodies included anti-Irga6 mouse monoclonal clone 10E7 antibody (7) at 1:10; anti-Irgb6 rabbit polyclonal antiserum (29) at 1:1000; anti-Gbp2 rabbit polyclonal antiserum (35) at 1:500, or anti-Gbp2 rabbit polyclonal antiserum (Jörn Coers, Duke University) at 1:1500 (these two Gbp2 antisera were used interchangeably with essentially identical results in all contexts), anti-GM130 mouse antibody (#612009, BD Transduction Laboratories) at 1:250, anti-TRAPα rabbit polyclonal antiserum (a gift of Chris Nicchitta, Duke University) at 1:125, anti-EEA1 mouse antibody (#610456, BD Transduction Laboratories) at 1:25, anti-proteasome 20 S C2 rabbit polyclonal antiserum (#ab3325, Abcam, Inc.) at 1:500, anti-p62/Sqstm1 rabbit polyclonal antiserum (#ab91526, Abcam, Inc.) at 1:500, anti-LC3 mouse monoclonal antibody (#M152–3, MBL International, Woburn, MA) at 1:50, and phalloidin-conjugated Alexa Fluor 488 (Molecular Probes/Invitrogen) at 1:40 (no secondary antibody used).

Images were collected on an Olympus IX70 microscope equipped with a Hamamatsu C8484–03G01 digital camera. Cells were magnified ×1000. Wide-field fluorescence images and z-stacks were collected using Metamorph 6.2.3.5. As mentioned in the text, images were, when appropriate, deconvolved using Auto Quant 9.3 software.

Colocalization Studies—Slides were prepared as described above and examined in phase contrast. One cell was randomly chosen from the field of view, and its thickness was determined. Z-stacks of the entire cell thickness with the appropriate two fluorescent channels were captured using Metamorph 6.2.3.5. Distance between planes was set at 0.3 microns. These two stacks were then flattened into two-dimensional representations using the three-dimensional reconstruction function of Metamorph and thresholded to remove background fluorescence. Thresholded channels were then overlaid. Once 10 thresholded and overlaid images were obtained per genotype, the number of overlapping puncta in each cell was quantified in a blinded fashion.

Western Blotting—Western blot analyses were performed according to standard protocols. In brief, lysates were boiled in SDS and separated on 8–16% gradient Tris-glycine gels (#EC60485, Invitrogen). Proteins were transferred overnight to Immobilon synthetic membranes (Millipore). Membranes were blocked in 5% (w/v) milk in TBS-Tween 20 for 60 min, then incubated in primary antibody for 60 min, washed, and incubated in secondary antibody for 60 min. Primary antibodies utilized include anti-Gbp2 rabbit polyclonal antiserum (Jörn Coers, Duke University) at 1:1000, anti-p62/Sqstm1 rabbit polyclonal antiserum (#ab91526, Abcam, Inc.) at 1:1000, anti-Irgm3 mouse monoclonal antibody (#610880, BD Transduction Laboratories) at 1:1000, and anti-actin clone C4 mouse monoclonal antibody (#MAB1501, Millipore) at 1:1500. Secondary antibodies used were goat anti-rabbit (H+L) HRP-conjugated IgG and goat anti-mouse (H+L) HRP-conjugated IgG (#AP307P and #AP308P, Millipore) at 1:1000. Blots were developed in SuperSignal west pico chemiluminescent substrate (#34708, Thermo Scientific, Rockford, IL) and imaged on a Kodak Image Station 4000R using Carestream Molecular Imaging software. Carestream software was also used to quantify sum intensities of bands.

TUBE 1 Pull-down of Polyubiquitinated Protein—Wild-type, Irgm1$^{-/-}$, and Irgm3$^{-/-}$ 3T3 cells were grown in 15-cm tissue culture dishes and exposed to 100 units/ml IFN-γ for 24 h prior to lysis. Cells were washed in PBS and lysed in 0.6 ml of lysis buffer (50 mM Tris-HCL (pH 7.4), 0.15 M NaCl, 1 mM EDTA, 1% Nonidet P-40, 10% glycerol). Input control samples were obtained by removing 0.2-ml aliquots and centrifuging at 16,000 × *g* at 4 °C for 5 min. Supernatants were mixed 3:1 with

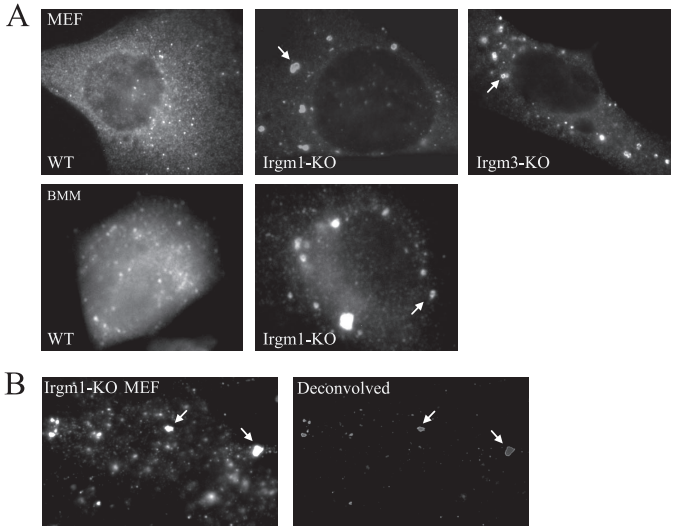

FIGURE 1. **Altered localization of Gbp2 in cells deficient for Irgm1 or Irgm3.** *A*, 3T3 MEFs or primary bone marrow macrophages of the indicated genotypes were activated with 100 units/ml IFN-γ for 24 h and then processed for immunostaining with anti-Gbp2 antibodies. Images were magnified ×1000. Shown is one representative of three experiments. Note the large ring-like structures denoted with *arrows*. *B*, Irgm1-deficient 3T3 MEFs were activated with 100 units/ml IFN-γ for 24 h and then processed for immunostaining with anti-Gbp2 antibodies. Z-stack images were obtained (*left panel*, *one plane*) and then deconvolved (*right panel*, *one plane*). Shown is one representative of three experiments. Ring-like structures are denoted with *arrows*. Images were magnified ×1000.

4× sample buffer containing 0.4 M DTT (Invitrogen). To assay for detergent-insoluble protein aggregates that might sediment during centrifugation, pellets were suspended in 0.2 ml of 1× sample buffer containing 0.1 M DTT. Viscosity of the pellet suspension was reduced by 10–15 passages through a 23-gauge needle attached to a 1-ml syringe. To keep aggregated proteins in the suspension, the lysates were not cleared by centrifugation. Agarose beads coupled to tandem ubiquitin binding entity 1 (TUBE 1, LifeSensors, Malvern, PA) or uncoupled beads were equilibrated in TBS-T (10mM Tris-HCl (pH 8.0), 0.15 M NaCl, 0.05% Tween 20) according to the supplier's recommendations. A sedimented bead volume of 30 μl was used per pull-down sample. Lysates were incubated with uncoupled agarose beads for 30 min at 4 °C. Beads were sedimented at low speed (700 × *g*), and the supernates were transferred to tubes containing TUBE 1-coupled beads. Incubation at 4 °C was continued for 1 h. Beads were sedimented and washed in TBS-T a total of four times. Beads were suspended in 1× sample buffer containing 0.1 M DTT. All samples were heated in a boiling water bath for 5 min prior to electrophoresis and Western blotting.

Immunoprecipitation Assay—For each immunoprecipitation, 50 μl of protein A-coupled paramagnetic beads (Dynabeads, Invitrogen) were isolated on a magnetic stand (Promega,

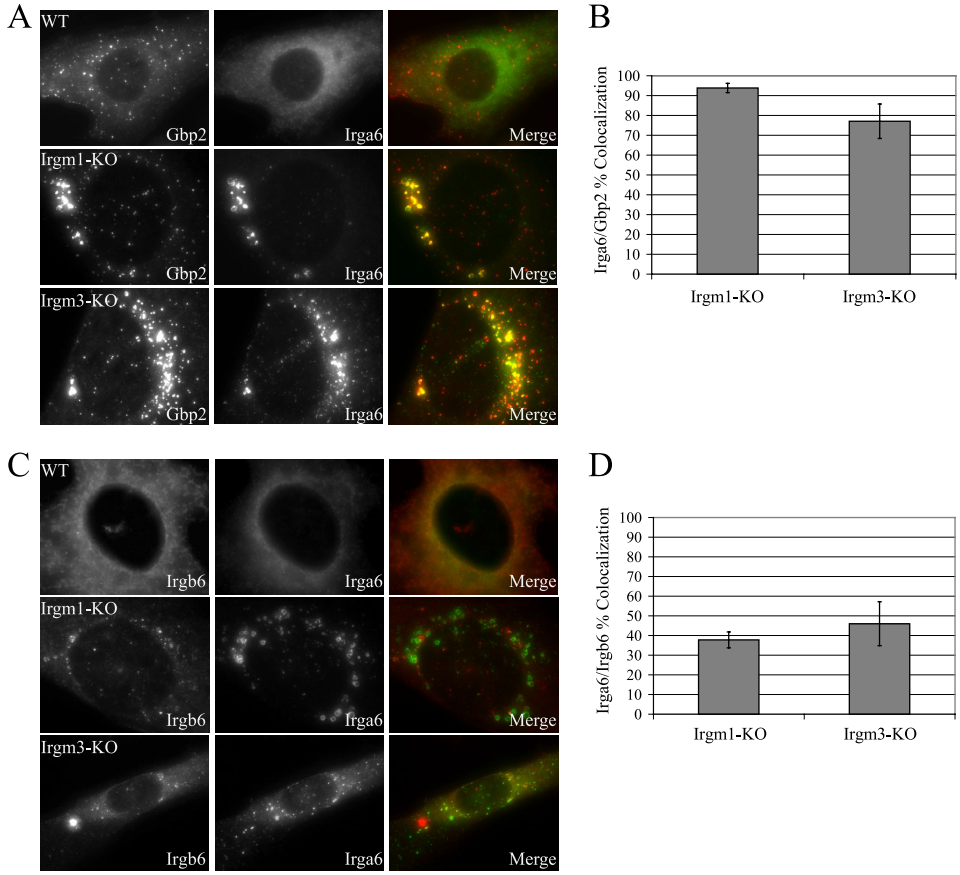

FIGURE 2. **Gbp2 colocalizes with GKS IRG proteins in IRGM-deficient cells.** 3T3 MEFs of the indicated genotypes were activated with 100 units/ml IFN-γ for 24 h and then processed for immunostaining with anti-Gbp2 and Irga6 antibodies (*A*) or anti-Irgb6 and Irga6 antibodies (*C*). Representative two-dimensional projections of z-stack images were magnified ×1000. Also displayed are the average percentage of Irga6 puncta colocalizing with Gbp2 puncta (*B*) or Irgb6 puncta (*D*). Puncta were scored in a blinded fashion in 10 cells per genotype. Note that wild-type cells were not analyzed because of the absence of Irga6 puncta. The *error bars* represent mean ± S.E. Differences between Irgm1- and Irgm3-deficient cells were not statistically significant ($p > 0.05$). Data are representative of three experiments.

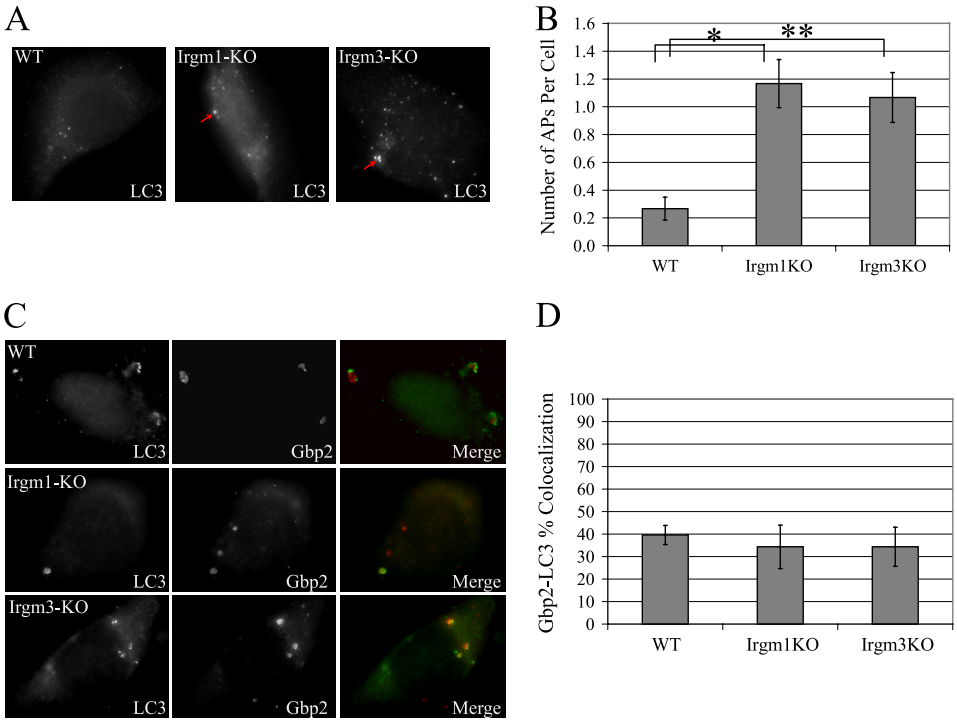

FIGURE 3. **IRGM deficiency leads to an increase in Gbp2-tagged autophagosome accumulation.** *A*, MEFs of the indicated genotypes were activated with IFN-γ for 24 h and then processed for immunostaining with anti-LC3 antibodies. Shown are representative two-dimensional projections of z-stack images that were magnified ×1000. Autophagosomes were defined as puncta or punctate structures that were both larger and more intense than background puncta and are marked with *arrows*. *B*, autophagosome (*AP*) number per cell was assessed in a blinded fashion in 10 cells per genotype per experiment. Shown are averages of three separate experiments. The *error bars* indicate mean ± S.E. *, $p = 2.69 \times 10^{-5}$; **, $p = 2.16 \times 10^{-4}$. *C*, MEFs of the indicated genotypes were activated with IFN-γ for 24 h and then processed for immunostaining with anti-LC3 and Gbp2 antibodies. Shown are representative two-dimensional projections of z-stack images that were magnified ×1000. *D*, LC3-Gbp2 colocalization was quantified from 10 cells per genotype. Differences between genotypes were not statistically significant ($p > 0.05$).

Madison, WI) and suspended in 0.2 ml of PBS containing 0.02% (v/v) Tween 20 (PBS-T). One microliter of either preimmune serum or anti-Irgm3 polyclonal antiserum (38) was added, and bead suspensions were incubated with rotation at room temperature for 20 min. Antibody-bound beads were washed once in PBS-T prior to addition of cell lysates. Wild-type, Irgm1$^{-/-}$, or Irgm3$^{-/-}$ 3T3 cells in 10-cm tissue culture dishes were given 100 units/ml IFN-γ for 24 h and lysed in PBS containing 1% (v/v) Nonidet P-40 and proteinase inhibitors (Calbiochem). 0.35 ml cell lysate with or without 0.5 mM GDP or GTPγS was added to the antibody-bound beads and incubated at room temperature for 20 min with rotation. Beads were magnetically separated and washed three times. Washed beads were removed to a fresh tube and suspended in 1× sample buffer (0.09 M DTT, 1.2% SDS, 0.012 M EDTA, 0.0025% bromphenol blue, 6% sucrose). Samples were heated to 100 °C to elute proteins and used for Western blotting. To minimize cross-reaction of the secondary antibody with eluted IgG, a secondary antibody that does not recognize denatured IgG (Clean Blot, Thermo Scientific) was used.

Statistical Analysis—Student's *t* test, as calculated by Excel, was used to assess statistical significance. The significance threshold was arbitrarily determined to be $p < 0.05$.

RESULTS

The Absence of Irgm1 or Irgm3 Affects the Localization of Gbp2—As mentioned above, we and others have previously demonstrated that the GMS IRG proteins Irgm1 and Irgm3 regulate the localization of GKS IRG proteins. The absence of Irgm1/m3 leads to the relocalization of Irga6 and Irgb6 from the endoplasmic reticulum and cytosol (7) into aggregate-like complexes. These effects were thought to be specific to IRG proteins, related to direct interactions between GMS and GKS proteins (30). In this study, we addressed whether the IRGM/GMS proteins affect broader processes that may affect the functioning of other proteins, including the GBPs. Absence of Irgm1 or Irgm3 in interferon-treated mouse fibroblasts or macrophages grossly altered distribution of Gbp2 from punctate cytoplasmic structures (presumably small vesicles to which Gbp2 has been purported to localize in previous studies (39)) to much larger, ring-like structures (Fig. 1). A hollow core was apparent in most of the Gbp2-positive structures, (Fig. 1, *arrows*), particularly in deconvolved images, suggesting that they could be membranous/vesicular. Costaining studies were also performed to determine whether GKS IRG proteins were concurrently present in the Gbp2-positive compartments (Fig. 2). Nearly all of the Gbp2-positive structures in Irgm1- and Irgm3-deficient cells also contained Irga6 (94 and 77%, respectively). In contrast, Irga6 and Irgb6 colocalized in only a fraction of the ring-like structures (38% in Irgm1-deficient cells and 46% in Irgm3-deficient cells), indicating that although the structures contained both GBPs and IRG proteins, there was some heterogeneity among them. Collectively, these data suggest that Irgm1 and Irgm3 regulate processes that control the transfer of GBP and IRG proteins from diverse initial locations within the cells to an overlapping set of large, ring-like compartments.

Gbp2 Partially Colocalizes with Autophagic Markers in the Absence of IRGM Proteins—In an attempt to identify the compartment to which Gbp2 localizes in the absence of Irgm1 or Irgm3, we undertook a variety of costaining studies. The Gbp2-positive structures did not colocalize with a number of markers for intracellular lipid compartments and for the cytoskeleton, including TRAP-α (endoplasmic reticulum), GM130 (Golgi), EEA1 (early endosomes), LAMP1 (late endosomes/lysosomes), mitotracker red (mitochondria), bodipy (lipid droplets), actin, tubulin, and vimentin (data not shown). Instead, we found that some Gbp2-positive structures were positive for LC3, an autophagic marker. Autophagy is a system of bulk protein degradation in which a double membrane forms around a portion of the cytoplasm, creating an autophagosome that fuses with late endosomes/lysosomes and becomes acidified, leading to the degradation of its contents. (For reviews, see Refs. 40–42.) This process serves not only as a survival mechanism during nutrient deprivation but also as a mechanism to remove intracellular pathogens (43). Several autophagy-related proteins are integral to the process, including LC3/Atg8, which, after activation by addition of phosphatidylethanolamine, localizes to the outer membrane of autophagosomes (44), and Atg5, which, when covalently bound to Atg12, is required for this modification of LC3 (45, 46). Importantly, previous studies have shown that Irgm1 may be involved in autophagy in a manner that has yet to be defined. Overexpression of Irgm1 in RAW 264.7 cells led to an increased number of autophagosomes, whereas knockdown of Irgm1 expression led to a decrease in IFN-γ-induced autophagosome number (24). In this study, autophagosomes were identified by LC3 immunostaining. In IFN-γ-activated Irgm1- and Irgm3-deficient cells, there was an increase in the number of large, intense LC3 puncta per cell relative to activated WT cells (Fig. 3, *A* and *B*), suggesting that IRGM deficiency leads to an increase in autophagosome levels, in contrast to the results of previous studies (24). In costaining studies, it was clear that Gbp2 ring-like structures colocalized with LC3 in WT, Irgm1-, and Irgm3-deficient cells, although it should be emphasized that very few of these structures were found in WT cells (Fig. 3, *C* and *D*). Although the Gbp2-positive structures were LC3-positive, they were not LAMP1-positive (data not shown), which suggests, along with data presented below, that these are likely immature or abortive autophagosomal structures. Finally, partial rings that were Gbp2-positive were commonly noted in Irgm1-deficient cells, indicating that Gbp2 may be acquired early during the process of autophagosome formation (data not shown).

Altered Autophagic Flux in the Absence of Irgm1—To explore whether the increase in autophagosome levels observed in IRGM-deficient cells was due to an increase in autophagosome formation or a decrease in autophagosome clearance, we examined levels of p62/Sqstm1 before and after interferon-γ treatment. Because p62 is a protein that is reliably degraded when brought to autophagosomes, levels of p62 are a useful surrogate to measure flux through the pathway (47). In the absence of Irgm1, p62 levels were increased in response to interferon treatment (Fig. 4*A*), indicating a deficiency in autophagic flux. Interestingly, p62 levels were not affected by Irgm3 deficiency (not shown), indicating that Irgm1 and Irgm3 function differently at some level to regulate autophagic protein degradation.

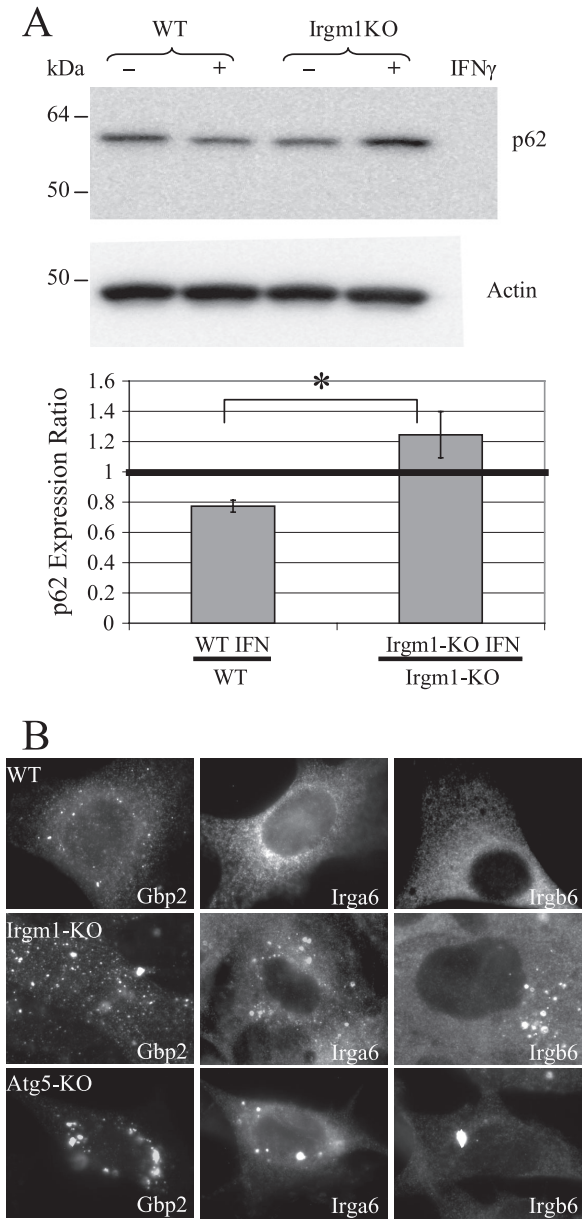

FIGURE 4. **Irgm1 deficiency leads to impaired autophagic flux.** *A*, MEFs of the indicated genotypes were or were not activated with IFN-γ for 24 h and then processed for Western blotting with anti-p62 antibodies. Shown is one representative of four experiments. The positions of molecular mass markers are shown at the left. p62 band sum intensities, normalized to actin, were calculated for all four experiments. Shown is the average ratio of interferon-γ treated p62 level to untreated p62 level for each genotype, calculated across four experiments. The *error bars* indicate mean ± S.E. *, $p = 0.0496$. *B*, MEFs of the indicated genotypes were activated with IFN-γ for 24 h and then processed for immunostaining with anti-Gbp2, Irga6, and Irgb6 antibodies. Images were magnified ×1000. Shown is one representative of three experiments.

To address this possibility further, we additionally blocked autophagic flux by a different method, Atg5-deficiency, to determine whether it would also lead to transfer of IRG and GBP proteins to autophagosomes. It has been previously shown that in Atg5-deficient cells, GKS IRG proteins have decreased protein levels and form aggregates (48, 49). We found this to be the case for Gbp2 as well, as absence of Atg5 in both fibroblasts

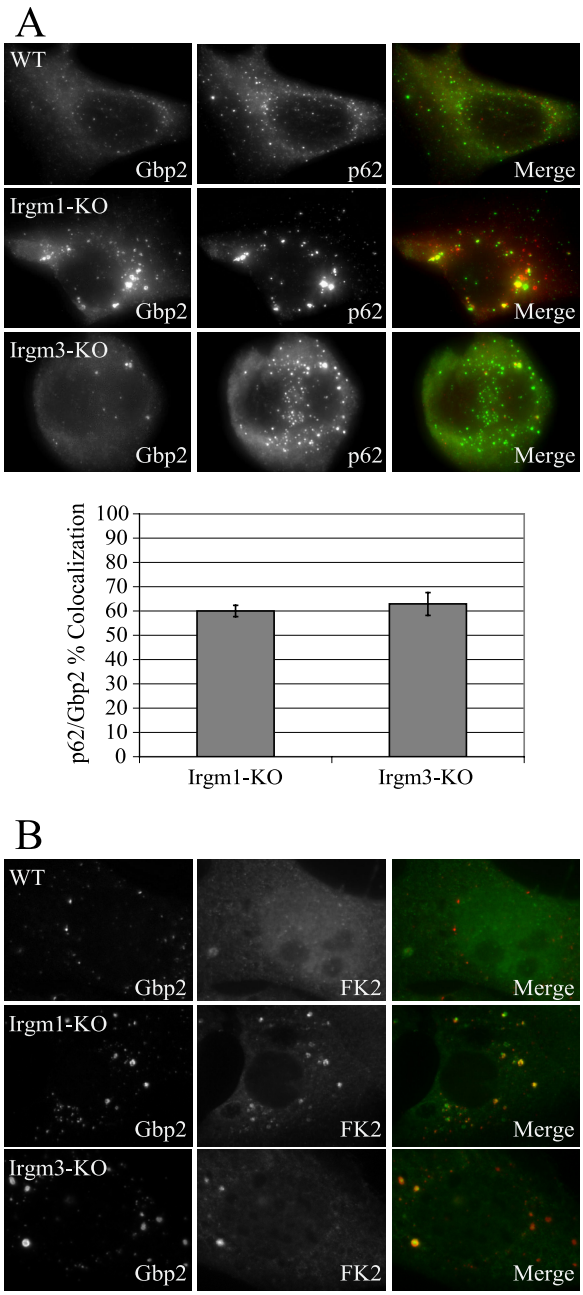

FIGURE 5. **IRGM deficiency leads to colocalization of Gbp2 with ubiquitin and p62.** MEFs of the indicated genotypes were activated with IFN-γ for 24 h and then processed for immunostaining with anti-p62 antibody (*A*) or FK2 (anti-ubiquitin) antibody (*B*). Shown are representative two-dimensional projections of z-stack images from three experiments. Images were magnified ×1000. Gbp2 ring-like structure and p62 puncta colocalization was quantified from 10 cells per genotype. The *error bars* indicate mean ± S.E. Differences between Irgm1- and Irgm3-deficient cells were not statistically significant ($p > 0.05$). Note that wild-type cells were not quantified because of the rarity of Gbp2 ring-like structures.

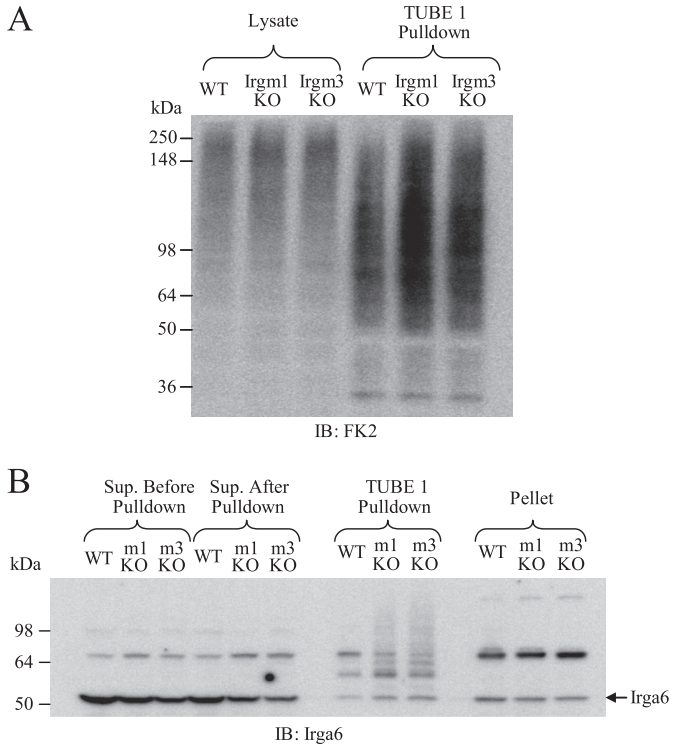

FIGURE 6. **IRGM deficiency leads to increased levels of Lys-63-ubiquitinated proteins, including Irga6.** Poly-Lys-63-ubiquitinated proteins were precipitated from IFN-γ-treated MEF lysates of the indicated genotypes using TUBE 1-conjugated resin. Proteins were separated by SDS-PAGE and blotted (*IB*) with FK2 (ubiquitin) antibodies (*A*) or Irga6 antibodies (*B*). Additional control samples taken included lysate before and after TUBE 1 addition and detergent-insoluble aggregates/excess membranous material pelleted before TUBE 1 addition. *Sup.*, supernatant. Shown is one representative of three experiments.

(Fig. 4*B*) and macrophages (not shown) led to the accumulation of large Gbp2-, Irgb6-, and Irga6-positive rings. These structures were even larger and more striking than those seen in Irgm1- or Irgm3-deficient cells, which implies that Irgm1/m3 deficiency leads to a partial block in autophagic flux as compared with a complete block in Atg5-deficient cells. The Gbp2 positive rings that accumulated in Atg5-deficient cells were not LC3-positive (data not shown). This is consistent with the role of Atg5 in lipidation and activation of LC3 but, importantly, contrasts with the LC3-positive Gbp2 rings seen in Irgm1-deficient cells. This implies that Irgm1 and Irgm3 influence autophagosomal flux at a point after LC3 acquisition on the autophagosome.

Ubiquitination of Irga6, but not Gbp2, in the Absence of Irgm1 or Irgm3—There are several mechanisms through which proteins may enter the autophagic pathway for degradation. One of these involves ubiquitination of targeted proteins, followed by their transfer to the autophagic system by an adapter protein called p62/Sqstm1 (50, 51). This protein binds both ubiquitin and the autophagosome outer membrane component LC3, physically bringing polyubiquitinated molecules to the forming autophagosome, with p62 eventually being degraded along with the other contents of the autophagosome (52, 53). To determine whether the presence of Irgm1 or Irgm3 was required for degradation of GKS IRG proteins through this pathway, we first performed costaining with anti-ubiquitin and anti-p62 antibodies, revealing that the Gbp2-positive structures (Fig. 5, *A* and *B*) and Irga6-positive structures (data not shown) seen in the absence of Irgm1 or Irgm3 are also positive for ubiquitin and p62. Polyubiquitin chains can be linked through any of seven lysines in the ubiquitin sequence, leading to chains with unique three-dimensional structures and characteristics (54). It has recently been shown that unlike the commonly studied Lys-48-linked polyubiquitin chains, Lys-63-linked polyubiquiti-

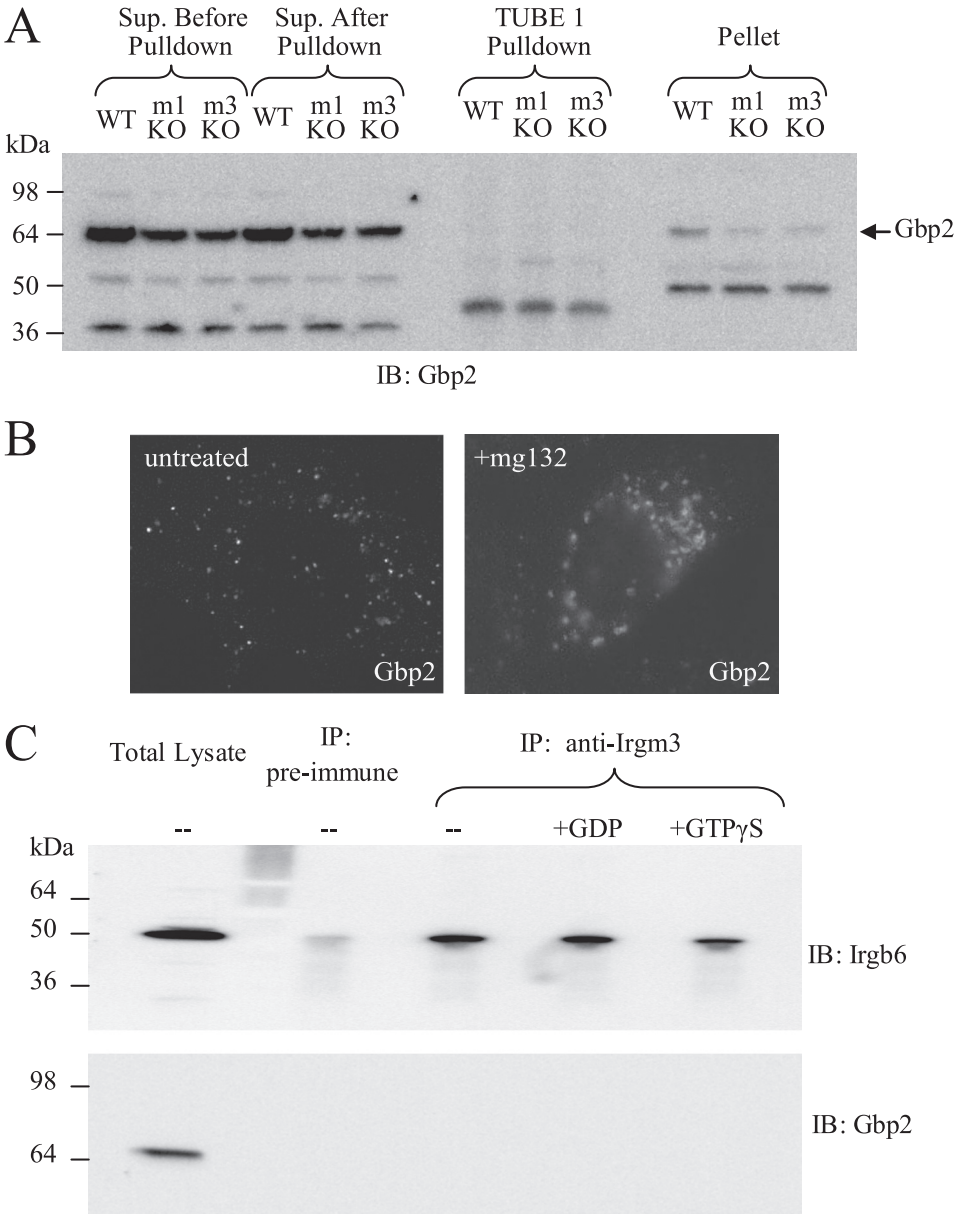

FIGURE 7. **Gbp2 localizes to autophagosomal structures independent of IRGM activity.** *A*, poly-Lys-63-ubiquitinated proteins were precipitated from IFN-γ treated MEF lysates of the indicated genotypes using TUBE 1. Proteins were separated by SDS-PAGE and blotted (*IB*) with Gbp2 antibody. Control samples taken included lysate before and after TUBE 1 addition and detergent-insoluble aggregates/excess membranous material pelleted before TUBE 1 addition. *Sup.*, supernatant. Shown is one representative of three experiments. *B*, wild-type MEFs were activated with IFN-γ for 24 h and simultaneously exposed to 10 μM MG132 or control conditions. Cells were then processed for immunostaining with anti-Gbp2 antibodies. Images were magnified ×1000. Shown are representative images from three studies. *C*, lysates were prepared from WT MEFs that had been activated with 100 units/ml IFN-γ for 24 h. The lysates were used for immunoprecipitation (*IP*) with anti-Irgm3 antibodies, followed by blotting with anti-Irgb6 or anti-Gbp2 antibodies, as indicated. In some cases, the lysates were loaded with 0.5 mM of the indicated guanine nucleotides prior to immunoprecipitation. Shown at the *left* are the positions of selected molecular weight markers. Data are representative of three experiments.

nated proteins are insensitive to degradation by the proteasome (55). Furthermore, depolarized mitochondria are decorated with Lys-63- and Lys-27-linked polyubiquitin chains, leading to selective autophagy of these organelles (56). These findings imply that Lys-63- and Lys-27-linked polyubiquitin tags may be signals for selective quality control autophagy. In this study, we utilized TUBE 1, a peptide designed to stabilize and identify polyubiquitinated proteins that has approximately a 10-fold higher affinity for Lys-63-linked polyubiquitin chains over Lys-48-linked chains, to examine levels of Lys-63 ubiquitination in IRGM-deficient cells. Total levels of Lys-63-linked polyubiquitinated proteins were increased in Irgm1- and Irgm3-deficient cells (Fig. 6*A*), indicating that there was a general block in removal of such proteins in these cells, consistent with the idea that IRGM proteins are required for normal autophagic clearance of IRG GKS proteins. Furthermore, TUBE 1 was able to precipitate protein species recognized by anti-Irga6 antiserum that were of higher molecular weight than Irga6 and likely represent ubiquitinated Irga6 (Fig. 6*B*). Apparent in the samples derived from Irgm1- and Irgm3-deficient cells was a ladder/smear that is typical of proteins in ubiquitin-positive inclusions (57), suggesting an increase in Lys-63-linked polyubiquitinated

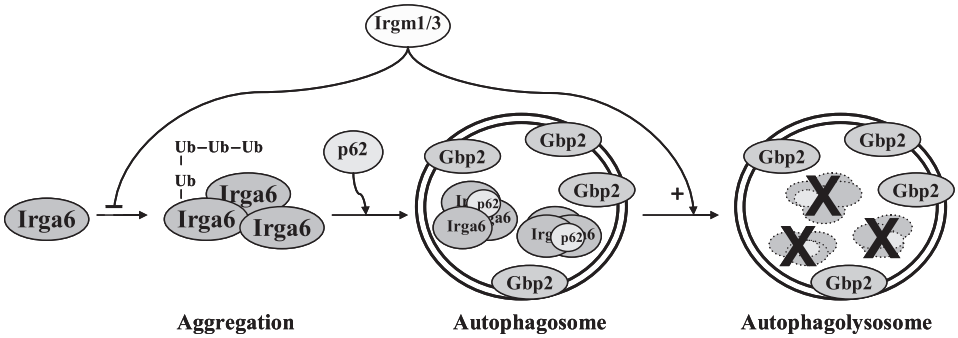

FIGURE 8. **Model of IRG and GBP involvement in autophagic protein degradation.** GKS IRGs, including Irga6, are prevented from aggregating by GMS IRGs, including Irgm1 and Irgm3. Excess GKS IRGs aggregate and are recognized by unknown factors and polyubiquitinated through Lys-63 linkages. Aggregates are then recognized by p62 and brought to autophagosomes, to which Gbp2 is also recruited. Formation and/or maturation of the structures is regulated by Irgm1 and Irgm3. During the process of maturation, ubiquitinated IRGs as well as p62 are degraded.

Irga6 in those cells. This finding thus implies that GKS IRG proteins form polyubiquitinated aggregates that are transferred via p62/Sqstm1 to the autophagic system for degradation.

Gbp2 May Play a Role in the Autophagic Processes—We also addressed whether Gbp2 was Lys-63-ubiquitinated using the TUBE 1 pull-down assay (Fig. 7*A*). In contrast to the results examining Irga6, no high molecular weight species identified by Gbp2 antibodies were found in the TUBE 1 pull-downs. This suggests that Gbp2 is not substantially Lys-63-ubiquitinated in wild-type, Irgm1-deficient, or Irgm3-deficient cells and thus might be found in autophagosomal structures not because it is being degraded but because it is itself involved in autophagy. To examine this theory, we induced quality control autophagy in wild-type cells by treatment with either of two proteasomal inhibitors, MG132 (Fig. 7*B*) and lactacystin (not shown). Inhibition of the proteasome has been shown previously to up-regulate autophagy as a compensatory degradation system (58). After treatment with either inhibitor in IFN-γ-activated wild-type cells, the normal vesicular localization pattern of Gbp2 was altered to ring-like structures, very similar to that noted in Irgm1-, Irgm3-, and Atg5-deficient cells. This indicates that Gbp2 localizes to autophagosomes when autophagy is induced, regardless of the presence or absence of IRGM proteins. Furthermore, although the absence of IRGM proteins influences Gbp2 localization, we find that Irgm3 does not directly interact with Gbp2 (Fig. 7*C*). Previous yeast two-hybrid and pull-down studies have shown that Irgm1 and Irgm3 can directly interact with other GKS IRG proteins, such as Irga6 and Irgb6, in a nucleotide-dependent fashion (30). These data have led to a model suggesting that IRGM proteins may hold other IRG proteins in inactive/GDP-bound conformations that prevent their oligomerization and the formation of protein aggregates. However, despite being readily able to coimmunoprecipitate Irgb6 and Irgm3 with the same nucleotide-dependent trends observed previously, we were unable to coimmunoprecipitate Gbp2 and Irgm3 (Fig. 7*C*). These results suggest that Gbp2 can localize to autophagosomes independent of GMS IRG protein function and thus may itself be involved in autophagic processes.

DISCUSSION

The IRGM subfamily of IRG proteins regulates the expression, localization, and function of proteins in the other IRG subfamilies. We have presented evidence here that in the absence of IRGM proteins autophagic flux is impaired, with broader effects on other immunity-related factors, including the guanylate-binding proteins, another family of interferon-stimulated GTPases. We have further shown that although IRGM protein deficiency does not alter Gbp2 ubiquitination, it apparently alters Lys-63-linked polyubiquitination of Irga6, which then localizes to Gbp2-positive autophagosomal structures. We thus propose the following model for autophagic maintenance of GKS IRG protein levels (Fig. 8). GKS IRG proteins are held in an inactive state by direct interactions with GMS IRGs, as proposed previously (30). Excess GKS IRG aggregates are recognized by unknown factors and are then polyubiquitinated through Lys-63 linkages. Polyubiquitinated aggregates are then recognized by p62/Sqstm1 and brought to Gbp2-positive autophagosomes, where they are degraded as driven by Irgm1 and Irgm3. It is likely that formation of Gbp2-positive autophagosomes containing ubiquitinated Irga6 occurs continuously at a low level, as we found that approximately 10% of wild-type MEFs contain at least one Irga6- and Gbp2-positive ring-like structure (data not shown). Nevertheless, in the absence of GMS IRG proteins, Irga6 and other GKS IRGs aggregate more strongly, leading to large numbers of autophagosomes containing polyubiquitinated Irga6 that are unable to mature in the absence of Irgm1 and Irgm3. Because the structures are LC3-positive, the block in autophagic flux caused by Irgm1/3 deficiency would seem to occur downstream of LC3 acquisition on the autophagosome.

The finding that the absence of GMS IRG proteins leads to an increase in large LC3-tagged structures seemingly contradicts a previous study (24) that found slightly but significantly fewer GFP-LC3-tagged structures in cells treated with Irgm1 siRNA. This discrepancy could be due to different methodologies or cell types utilized (RAW 264.7 cells in Ref. 24 *versus* MEFs in our study). An additional explanation is that autophagy could be particularly sensitive to Irgm1 levels so that small changes in Irgm1 concentrations produced by the partial knockdown through siRNA *versus* the complete absence in the knockout may have differential impacts. The two studies do reach the same overall conclusion that Irgm1 activity promotes autophagy.

Several lines of data support our contention that the Gbp2-positive ring-like structures that accumulate in the cell are immature autophagosomal structures. First, they contain ubiquitinated Irga6 and are both LC3- and p62-positive. However, they do not appear to be fully mature, as they are LAMP1-negative. Further, they are not classic aggresomes as they lack several features of classic aggresomes (59). Classic aggresomes are typically surrounded by a vimentin cage, whereas this cage is lacking in the Irgm1/3-regulated structures; classic aggresomes are localized near the microtubule organizing center of the cells, whereas the Irgm1/3-regulated structures do not demonstrate this restricted localization; and classic aggresomes occur at one per cell, whereas several of the Irgm1/m3-regulated structures were often found in a single cell (data not shown). Thus, our data support the notion that these structures are immature or abortive autophagosomal structures that are not being efficiently removed from the cell, ostensibly because of the absence of Irgm1/3 activity.

Our data also define a clear distinction between the way in which IRGM proteins affect Gbp2 and GKS IRG proteins. The latter, represented by Irga6 in our studies, may be ubiquitinated through Lys-63 linkages, as suggested by the TUBE 1 pull-down studies. In absence of Irgm1 or Irgm3, the amount of ubiquitinated Irga6 that accumulates in cells increases substantially, presumably because of lack of efficient removal through Irgm1/3-driven autophagy. In contrast, our studies suggest that there is little ubiquitinated Gbp2 in IFN-γ-activated cells, whether wild-type or lacking Irgm1 or Irgm3. This suggests that Gbp2 is recruited to autophagosomes in the absence of Irgm1 or Irgm3, not as a protein targeted for degradation by autophagy but perhaps as a protein that is involved in the autophagic process itself. This contention is also supported by the accumulation of Gbp2-decorated structures in Atg5-deficient cells, similar to those seen in Irgm1/3-deficient cells, as well as Gbp2 accumulation on autophagosomes found in MG132-treated cells. Future work should clarify the mechanism whereby IRGM proteins and GBPs affect autophagic flux and the importance of this pathway in cell autonomous immune responses to intracellular infection.

REFERENCES

1. de Veer, M. J., Holko, M., Frevel, M., Walker, E., Der, S., Paranjape, J. M., Silverman, R. H., and Williams, B. R. (2001) *J. Leukocyte Biol.* **69,** 912–920
2. Ehrt, S., Schnappinger, D., Bekiranov, S., Drenkow, J., Shi, S., Gingeras, T. R., Gaasterland, T., Schoolnik, G., and Nathan, C. (2001) *J. Exp. Med.* **194,** 1123–1140
3. Halonen, S. K., Woods, T., McInnerney, K., and Weiss, L. M. (2006) *J. Neuroimmunol.* **175,** 19–30
4. Kota, R. S., Rutledge, J. C., Gohil, K., Kumar, A., Enelow, R. I., and Ramana, C. V. (2006) *Biochem. Biophys. Res. Commun.* **342,** 1137–1146
5. Uthaiah, R. C., Praefcke, G. J., Howard, J. C., and Herrmann, C. (2003) *J. Biol. Chem.* **278,** 29336–29343
6. Taylor, G. A., Stauber, R., Rulong, S., Hudson, E., Pei, V., Pavlakis, G. N., Resau, J. H., and Vande Woude, G. F. (1997) *J. Biol. Chem.* **272,** 10639–10645
7. Martens, S., Sabel, K., Lange, R., Uthaiah, R., Wolf, E., and Howard, J. C. (2004) *J. Immunol.* **173,** 2594–2606
8. Butcher, B. A., Greene, R. I., Henry, S. C., Annecharico, K. L., Weinberg, J. B., Denkers, E. Y., Sher, A., and Taylor, G. A. (2005) *Infect. Immun.* **73,** 3278–3286
9. Ghosh, A., Uthaiah, R., Howard, J., Herrmann, C., and Wolf, E. (2004) *Mol. Cell* **15,** 727–739
10. Danino, D., and Hinshaw, J. E. (2001) *Curr. Opin Cell Biol.* **13,** 454–460
11. Praefcke, G. J., and McMahon, H. T. (2004) *Nat. Rev. Mol. Cell Biol.* **5,** 133–147
12. Schafer, D. A. (2004) *Traffic* **5,** 463–469
13. Martens, S., Parvanova, I., Zerrahn, J., Griffiths, G., Schell, G., Reichmann, G., and Howard, J. C. (2005) *PLoS Pathog.* **1,** e24
14. Bekpen, C., Hunn, J. P., Rohde, C., Parvanova, I., Guethlein, L., Dunn, D. M., Glowalla, E., Leptin, M., and Howard, J. C. (2005) *Genome Biol.* **6,** R92
15. Boehm, U., Guethlein, L., Klamp, T., Ozbek, K., Schaub, A., Fütterer, A., Pfeffer, K., and Howard, J. C. (1998) *J. Immunol.* **161,** 6715–6723
16. de Souza, A. P., Tang, B., Tanowitz, H. B., Factor, S. M., Shtutin, V., Shirani, J., Taylor, G. A., Weiss, L. M., and Jelicks, L. A. (2003) *J. Parasitol.* **89,** 1237–1239
17. Feng, C. G., Weksberg, D. C., Taylor, G. A., Sher, A., and Goodell, M. A. (2008) *Cell Stem Cell* **2,** 83–89
18. Collazo, C. M., Yap, G. S., Hieny, S., Caspar, P., Feng, C. G., Taylor, G. A., and Sher, A. (2002) *Infect. Immun.* **70,** 6933–6939
19. Collazo, C. M., Yap, G. S., Sempowski, G. D., Lusby, K. C., Tessarollo, L., Woude, G. F., Sher, A., and Taylor, G. A. (2001) *J. Exp. Med.* **194,** 181–188
20. Feng, C. G., Collazo-Custodio, C. M., Eckhaus, M., Hieny, S., Belkaid, Y., Elkins, K., Jankovic, D., Taylor, G. A., and Sher, A. (2004) *J. Immunol.* **172,** 1163–1168
21. MacMicking, J. D., Taylor, G. A., and McKinney, J. D. (2003) *Science* **302,** 654–659
22. Taylor, G. A., Collazo, C. M., Yap, G. S., Nguyen, K., Gregorio, T. A., Taylor, L. S., Eagleson, B., Secrest, L., Southon, E. A., Reid, S. W., Tessarollo, L., Bray, M., McVicar, D. W., Komschlies, K. L., Young, H. A., Biron, C. A., Sher, A., and Vande Woude, G. F. (2000) *Proc. Natl. Acad. Sci. U.S.A.* **97,** 751–755
23. Gutierrez, M. G., Master, S. S., Singh, S. B., Taylor, G. A., Colombo, M. I., and Deretic, V. (2004) *Cell* **119,** 753–766
24. Singh, S. B., Davis, A. S., Taylor, G. A., and Deretic, V. (2006) *Science* **313,** 1438–1441
25. Henry, S. C., Daniell, X., Indaram, M., Whitesides, J. F., Sempowski, G. D., Howell, D., Oliver, T., and Taylor, G. A. (2007) *J. Immunol.* **179,** 6963–6972
26. Taylor, G. A. (2007) *Cell. Microbiol.* **9,** 1099–1107
27. Coers, J., Bernstein-Hanley, I., Grotsky, D., Parvanova, I., Howard, J. C., Taylor, G. A., Dietrich, W. F., and Starnbach, M. N. (2008) *J. Immunol.* **180,** 6237–6245
28. Vignola, M. J., Kashatus, D. F., Taylor, G. A., Counter, C. M., and Valdivia, R. H. *J. Biol. Chem.* **285,** 21625–21635
29. Henry, S. C., Daniell, X. G., Burroughs, A. R., Indaram, M., Howell, D. N., Coers, J., Starnbach, M. N., Hunn, J. P., Howard, J. C., Feng, C. G., Sher, A., and Taylor, G. A. (2009) *J. Leukocyte Biol.* **85,** 877–885
30. Hunn, J. P., Koenen-Waisman, S., Papic, N., Schroeder, N., Pawlowski, N., Lange, R., Kaiser, F., Zerrahn, J., Martens, S., and Howard, J. C. (2008) *EMBO J.* **27,** 2495–2509
31. Gupta, S. L., Rubin, B. Y., and Holmes, S. L. (1979) *Proc. Natl. Acad. Sci. U.S.A.* **76,** 4817–4821
32. Cheng, Y. S., Colonno, R. J., and Yin, F. H. (1983) *J. Biol. Chem.* **258,** 7746–7750
33. Kresse, A., Konermann, C., Degrandi, D., Beuter-Gunia, C., Wuerthner, J., Pfeffer, K., and Beer, S. (2008) *BMC Genomics* **9,** 158
34. Prakash, B., Praefcke, G. J., Renault, L., Wittinghofer, A., and Herrmann, C. (2000) *Nature* **403,** 567–571
35. Degrandi, D., Konermann, C., Beuter-Gunia, C., Kresse, A., Würthner, J., Kurig, S., Beer, S., and Pfeffer, K. (2007) *J. Immunol.* **179,** 7729–7740
36. Tietzel, I., El-Haibi, C., and Carabeo, R. A. (2009) *PLoS ONE* **4,** e6499
37. Todaro, G. J., and Green, H. (1963) *J. Cell Biol.* **17,** 299–313
38. Taylor, G. A., Jeffers, M., Largaespada, D. A., Jenkins, N. A., Copeland, N. G., and Woude, G. F. (1996) *J. Biol. Chem.* **271,** 20399–20405
39. Vestal, D. J., Gorbacheva, V. Y., and Sen, G. C. (2000) *J. Interferon Cytokine Res.* **20,** 991–1000
40. Kroemer, G., Mariño, G., and Levine, B. (2010) *Mol. Cell* **40,** 280–293
41. Simonsen, A., and Tooze, S. A. (2009) *J. Cell Biol.* **186,** 773–782

42. Yang, Z., and Klionsky, D. J. (2010) *Curr. Opin Cell Biol.* **22,** 124–131
43. Levine, B. (2005) *Cell* **120,** 159–162
44. Ichimura, Y., Kirisako, T., Takao, T., Satomi, Y., Shimonishi, Y., Ishihara, N., Mizushima, N., Tanida, I., Kominami, E., Ohsumi, M., Noda, T., and Ohsumi, Y. (2000) *Nature* **408,** 488–492
45. Mizushima, N., Noda, T., Yoshimori, T., Tanaka, Y., Ishii, T., George, M. D., Klionsky, D. J., Ohsumi, M., and Ohsumi, Y. (1998) *Nature* **395,** 395–398
46. Mizushima, N., Yamamoto, A., Hatano, M., Kobayashi, Y., Kabeya, Y., Suzuki, K., Tokuhisa, T., Ohsumi, Y., and Yoshimori, T. (2001) *J. Cell Biol.* **152,** 657–668
47. Klionsky, D. J., Abeliovich, H., Agostinis, P., Agrawal, D. K., Aliev, G., Askew, D. S., Baba, M., Baehrecke, E. H., Bahr, B. A., Ballabio, A., Bamber, B. A., Bassham, D. C., Bergamini, E., Bi, X., Biard-Piechaczyk, M., Blum, J. S., Bredesen, D. E., Brodsky, J. L., Brumell, J. H., Brunk, U. T., Bursch, W., Camougrand, N., Cebollero, E., Cecconi, F., Chen, Y., Chin, L. S., Choi, A., Chu, C. T., Chung, J., Clarke, P. G., Clark, R. S., Clarke, S. G., Clavé, C., Cleveland, J. L., Codogno, P., Colombo, M. I., Coto-Montes, A., Cregg, J. M., Cuervo, A. M., Debnath, J., Demarchi, F., Dennis, P. B., Dennis, P. A., Deretic, V., Devenish, R. J., Di Sano, F., Dice, J. F., Difiglia, M., Dinesh-Kumar, S., Distelhorst, C. W., Djavaheri-Mergny, M., Dorsey, F. C., Dröge, W., Dron, M., Dunn, W. A., Jr., Duszenko, M., Eissa, N. T., Elazar, Z., Esclatine, A., Eskelinen, E. L., Fésüs, L., Finley, K. D., Fuentes, J. M., Fueyo, J., Fujisaki, K., Galliot, B., Gao, F. B., Gewirtz, D. A., Gibson, S. B., Gohla, A., Goldberg, A. L., Gonzalez, R., González-Estévez, C., Gorski, S., Gottlieb, R. A., Häussinger, D., He, Y. W., Heidenreich, K., Hill, J. A., Høyer-Hansen, M., Hu, X., Huang, W. P., Iwasaki, A., Jäättelä, M., Jackson, W. T., Jiang, X., Jin, S., Johansen, T., Jung, J. U., Kadowaki, M., Kang, C., Kelekar, A., Kessel, D. H., Kiel, J. A., Kim, H. P., Kimchi, A., Kinsella, T. J., Kiselyov, K., Kitamoto, K., Knecht, E., Komatsu, M., Kominami, E., Kondo, S., Kovács, A. L., Kroemer, G., Kuan, C. Y., Kumar, R., Kundu, M., Landry, J., Laporte, M., Le, W., Lei, H. Y., Lenardo, M. J., Levine, B., Lieberman, A., Lim, K. L., Lin, F. C., Liou, W., Liu, L. F., Lopez-Berestein, G., López-Otín, C., Lu, B., Macleod, K. F., Malorni, W., Martinet, W., Matsuoka, K., Mautner, J., Meijer, A. J., Meléndez, A., Michels, P., Miotto, G., Mistiaen, W. P., Mizushima, N., Mograbi, B., Monastyrska, I., Moore, M. N., Moreira, P. I., Moriyasu, Y., Motyl, T., Münz, C., Murphy, L. O., Naqvi, N. I., Neufeld, T. P., Nishino, I., Nixon, R. A., Noda, T., Nürnberg, B., Ogawa, M., Oleinick, N. L., Olsen, L. J., Ozpolat, B., Paglin, S., Palmer, G. E., Papassideri, I., Parkes, M., Perlmutter, D. H., Perry, G., Piacentini, M., Pinkas-Kramarski, R., Prescott, M., Proikas-Cezanne, T., Raben, N., Rami, A., Reggiori, F., Rohrer, B., Rubinsztein, D. C., Ryan, K. M., Sadoshima, J., Sakagami, H., Sakai, Y., Sandri, M., Sasakawa, C., Sass, M., Schneider, C., Seglen, P. O., Seleverstov, O., Settleman, J., Shacka, J. J., Shapiro, I. M., Sibirny, A., Silva-Zacarin, E. C., Simon, H. U., Simone, C., Simonsen, A., Smith, M. A., Spanel-Borowski, K., Srinivas, V., Steeves, M., Stenmark, H., Stromhaug, P. E., Subauste, C. S., Sugimoto, S., Sulzer, D., Suzuki, T., Swanson, M. S., Tabas, I., Takeshita, F., Talbot, N. J., Tallóczy, Z., Tanaka, K., Tanaka, K., Tanida, I., Taylor, G. S., Taylor, J. P., Terman, A., Tettamanti, G., Thompson, C. B., Thumm, M., Tolkovsky, A. M., Tooze, S. A., Truant, R., Tumanovska, L. V., Uchiyama, Y., Ueno, T., Uzcátegui, N. L., van der Klei, I., Vaquero, E. C., Vellai, T., Vogel, M. W., Wang, H. G., Webster, P., Wiley, J. W., Xi, Z., Xiao, G., Yahalom, J., Yang, J. M., Yap, G., Yin, X. M., Yoshimori, T., Yu, L., Yue, Z., Yuzaki, M., Zabirnyk, O., Zheng, X., Zhu, X., and Deter, R. L. (2008) *Autophagy* **4,** 151–175
48. Zhao, Z., Fux, B., Goodwin, M., Dunay, I. R., Strong, D., Miller, B. C., Cadwell, K., Delgado, M. A., Ponpuak, M., Green, K. G., Schmidt, R. E., Mizushima, N., Deretic, V., Sibley, L. D., and Virgin, H. W. (2008) *Cell Host Microbe* **4,** 458–469
49. Khaminets, A., Hunn, J. P., Konen-Waisman, S., Zhao, Y. O., Preukschat, D., Coers, J., Boyle, J. P., Ong, Y. C., Boothroyd, J. C., Reichmann, G., and Howard, J. C. *Cell. Microbiol.* **12,** 939–961
50. Bjørkøy, G., Lamark, T., Brech, A., Outzen, H., Perander, M., Overvatn, A., Stenmark, H., and Johansen, T. (2005) *J. Cell Biol.* **171,** 603–614
51. Komatsu, M., Waguri, S., Koike, M., Sou, Y. S., Ueno, T., Hara, T., Mizushima, N., Iwata, J., Ezaki, J., Murata, S., Hamazaki, J., Nishito, Y., Iemura, S., Natsume, T., Yanagawa, T., Uwayama, J., Warabi, E., Yoshida, H., Ishii, T., Kobayashi, A., Yamamoto, M., Yue, Z., Uchiyama, Y., Kominami, E., and Tanaka, K. (2007) *Cell* **131,** 1149–1163
52. Ichimura, Y., Kumanomidou, T., Sou, Y. S., Mizushima, T., Ezaki, J., Ueno, T., Kominami, E., Yamane, T., Tanaka, K., and Komatsu, M. (2008) *J. Biol. Chem.* **283,** 22847–22857
53. Pankiv, S., Clausen, T. H., Lamark, T., Brech, A., Bruun, J. A., Outzen, H., Øvervatn, A., Bjørkøy, G., and Johansen, T. (2007) *J. Biol. Chem.* **282,** 24131–24145
54. Clague, M. J., and Urbé, S. (2010) *Cell* **143,** 682–685
55. Jacobson, A. D., Zhang, N. Y., Xu, P., Han, K. J., Noone, S., Peng, J., and Liu, C. W. (2009) *J. Biol. Chem.* **284,** 35485–35494
56. Geisler, S., Holmström, K. M., Skujat, D., Fiesel, F. C., Rothfuss, O. C., Kahle, P. J., and Springer, W. (2010) *Nat. Cell Biol.* **12,** 119–131
57. Waguri, S., and Komatsu, M. (2009) *Methods Enzymol.* **453,** 181–196
58. Pandey, U. B., Nie, Z., Batlevi, Y., McCray, B. A., Ritson, G. P., Nedelsky, N. B., Schwartz, S. L., DiProspero, N. A., Knight, M. A., Schuldiner, O., Padmanabhan, R., Hild, M., Berry, D. L., Garza, D., Hubbert, C. C., Yao, T. P., Baehrecke, E. H., and Taylor, J. P. (2007) *Nature* **447,** 859–863
59. Johnston, J. A., Ward, C. L., and Kopito, R. R. (1998) *J. Cell Biol.* **143,** 1883–1898